

NTC Thermistors of Y-Al-Mn-Fe-Ni-Cr-O Ceramics for Wide Temperature Range Measurement

Woonyoung Lee and Jinseong Park
Dept. of Materials and Engineering Chosun University
309 Seosuk-Dong, Gwangju 501-759, South Korea
lwyl1@hahafos.com, jsepark@chosun.ac.kr

Abstract— NTC thermistors of Y-Al-Mn-Fe-Ni-Cr-O systems were fabricated by using normal ceramic processing for wide temperature range measurement. Pt-Rh alloy as electrodes was inserted into the body during the forming process to increase the reliability of high temperature and to decrease the contact resistance. The properties were analyzed by XRD, SEM and resistance measurement. There are no distinct XRD patterns between $Y_{0.2}Al_{0.1}Mn_{0.27}Fe_{0.16}Ni_{0.27}O_x$ and $Y_{0.2}Al_{0.1}Mn_{0.264}Fe_{0.16}Ni_{0.264}Cr_{0.012}O_x$ because of too small content of Cr_2O_3 , as a dopant, to make peak difference or new phases within the XRD resolution. SEM images and resistance behaviors show the different properties. With the addition of Cr_2O_3 as a dopant, the crystallinity and the grain size were decreased and increased, respectively. The resistance behaviors were similar but the values are low with Cr_2O_3 . The specimens show the straight line relationship between the electrical resistivity and the temperature over a wide temperature range, indicating NTC thermistor characteristics.

Keywords- NTC thermistor; microstructure; wide temperature range; electrical resistance

I. INTRODUCTION

Negative temperature coefficient (NTC) thermistors are thermally sensitive resistors whose resistance decreases with increasing temperature [1-4]. They are mainly used in electronics for the suppression of in-rush current, for temperature measurement and control, and for compensation for other circuit elements [5-6].

The measurement range from low- to high-temperature is entirely insufficient for common ceramic thermistors because the coefficient of temperature sensitivity (or B constant) is usually high, over 4500K. Thus, the thermistors are classified by the room temperature applications below 100°C and the medium temperature applications between 100 °C and 300 °C.

Especially in the application of automobile and spaceship, it is necessary to measure a wide range from room temperature to very high temperature. Thermistors for these applications have to the value of hundreds of kΩ at room temperature and several decades of Ω at 900 °C. To purpose these goals, the researches have to focus to find a materials which has the low B constant, the linearity in the wide temperature range and the stable property and phase at high temperature.

Previously, the researches on NTC thermistors were predominantly focused on spinel or spinel-like structure. Those most used in practice are based on solid solutions of transition metal oxides, such as Mn_3O_4 , Co_3O_4 , and NiO , with the general formula AB_2O_4 . However, their application is commonly limited to temperatures below 200 °C [7-12]. Feltz and Polzl have proposed a system of compositions $Fe_xNi_yMn_{3-x-y}O_4$ based on the spinel structure for high temperature applications [13]. Yet B constants are not stable for temperatures below 400 °C, which limits the temperature range for applications. In the special application, ZrO_2 and Y_2O_3 thermistor could be used only at high temperature above 500 °C because of too high resistance below 300 °C.

Oxide ceramic semiconductors based on the perovskite type structure are expected to be more available to measure wide temperature range from low- to high-temperature [14-15]. Relatively high conductivity values and low activation energies or even metallic behavior are often found for perovskites. PTC ceramics based on acceptor doping, e.g. by substitution of Fe^{3+} for Ti^{4+} in the composition of $SrTi_{1-x}Fe_xO_3$ perovskite structure provide a low or zero B constant over 550 °C [16-18]. $LaCoO_3$ has a room-temperature conductivity with metallic behavior above 330 °C [19-20].

Y_2O_3 and Al_2O_3 are well known refractory material and have high resistance at high temperature. The transition metal oxides like MnO_2 , Fe_2O_3 , NiO and Cr_2O_3 are known the composition for room temperature thermistor. Thus, it could be possible to establish a wide range thermistor by the mixture of transition metal oxides and refractory material like Al_2O_3 and Y_2O_3 . It is thus required to expand the selection of suitable composition with the desired electrical properties for wide temperature range measurement. In the present study, the microstructure and electrical properties of Y-Al-Mn-Fe-Ni-Cr-O system were studied on NTC thermistor for wide temperature applications.

II. EXPERIMENTS

Y_2O_3 , Al_2O_3 , MnO_2 , Fe_2O_3 , NiO , and Cr_2O_3 powders with high-purity ($\geq 99.5\%$) were used as the chemical reagents to establish a wide range thermistors. These powders were weighed for the composition of $Y_{0.2}Al_{0.1}Mn_{0.27}Fe_{0.16}Ni_{0.27}O_x$ and $Y_{0.2}Al_{0.1}Mn_{0.264}Fe_{0.16}Ni_{0.264}Cr_{0.012}O_x$.

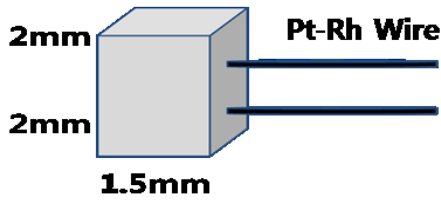


Figure 1. Specimen size and the structure of electrodes inserted into the specimen.

The wet-blending was performed by ball-milling of the mixtures of weighed powders for 12 h. The wet-blended mixtures were dried at 120 °C for 24 h. The mixture was subsequently calcined at 1200 °C with a heating rate of 5 °C/min for dwell time of 2 h.

The sintered mass was again crushed and pulverized to obtain the fine powder. Subsequently, the fine powders were pressed at 120 MPa into a rectangular mold. The size of green pellet is 2 mm x 1.5 mm x 2 mm and it has a pair of inserted Pt-Rh (13%) wires as electrodes as shown in Fig. 1. The diameter of Pt-Rh electrode is 0.30 mm. The distance between 2 wires and the inserting depth into the pellet are 1 mm.

The pellets were co-sintered, ceramic body and Pt-Rh metals, at 1400°C for 1 h in air atmosphere. The crystal structure of the as-sintered specimens was analyzed with X-ray diffraction (XRD) (Rigaku DMAX 2500) using Cu K α (0.15406 nm) radiation at 40 kV and 25 mA. The XRD patterns were obtained over the range of 10 ~ 70° 2 θ . The changes in microstructures of the as-sintered specimens were investigated by using a field emission scanning electron microscope (FESEM; Hitachi S-4700). The electrical resistance as a function of temperature for the as-sintered specimens was measured by using a digital multi-meter (hp34401B).

III. RESULTS AND DISCUSSION

The XRD patterns of $Y_{0.2}Al_{0.1}Mn_{0.27}Fe_{0.16}Ni_{0.27}O_x$ with or without 0.012mol Cr_2O_3 as a dopant were shown in Figure 2. The new phases were formed after sintering at 1400 °C for 1 h. Compared to the each unit powder after sintering, the similar XRD peaks were detected and it is known the perovskite phase and others. There are no peak differences between them because the amount of Cr_2O_3 is too small to make peak differences or new phases within the XRD resolution.

The SEM images obtained from the cross section of $Y_{0.2}Al_{0.1}Mn_{0.27}Fe_{0.16}Ni_{0.27}O_x$ and $Y_{0.2}Al_{0.1}Mn_{0.264}Fe_{0.16}Ni_{0.264}Cr_{0.012}O_x$ were shown in Fig.3. Although it is difficult to find a difference of XRD peaks as shown Figure 2, the SEM image clearly different from the addition of small content of 0.01mol Cr_2O_3 . The SEM image shows a sharp crystal plane in the case of non doped Cr_2O_3 , $Y_{0.2}Al_{0.1}Mn_{0.27}Fe_{0.16}Ni_{0.27}O_x$. However, it is difficult to find a sharp crystal plane for $Y_{0.2}Al_{0.1}Mn_{0.264}Fe_{0.16}Ni_{0.264}Cr_{0.012}O_x$ with the dopant of 0.013mol Cr_2O_3 . The grain sizes of non doped Cr_2O_3 as shown in Figure 3(a) is smaller than those of doped Cr_2O_3 as shown in Figure 3(b).

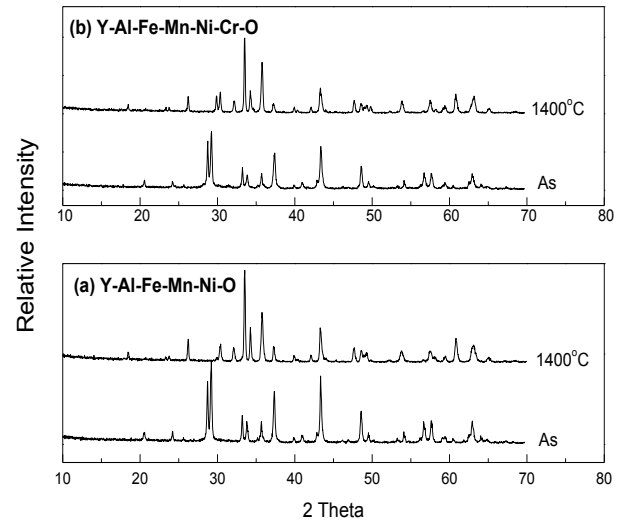


Figure 2. The XRD patterns of (a) $Y_{0.2}Al_{0.1}Mn_{0.27}Fe_{0.16}Ni_{0.27}O_x$ and (b) $Y_{0.2}Al_{0.1}Mn_{0.264}Fe_{0.16}Ni_{0.264}Cr_{0.012}O_x$.

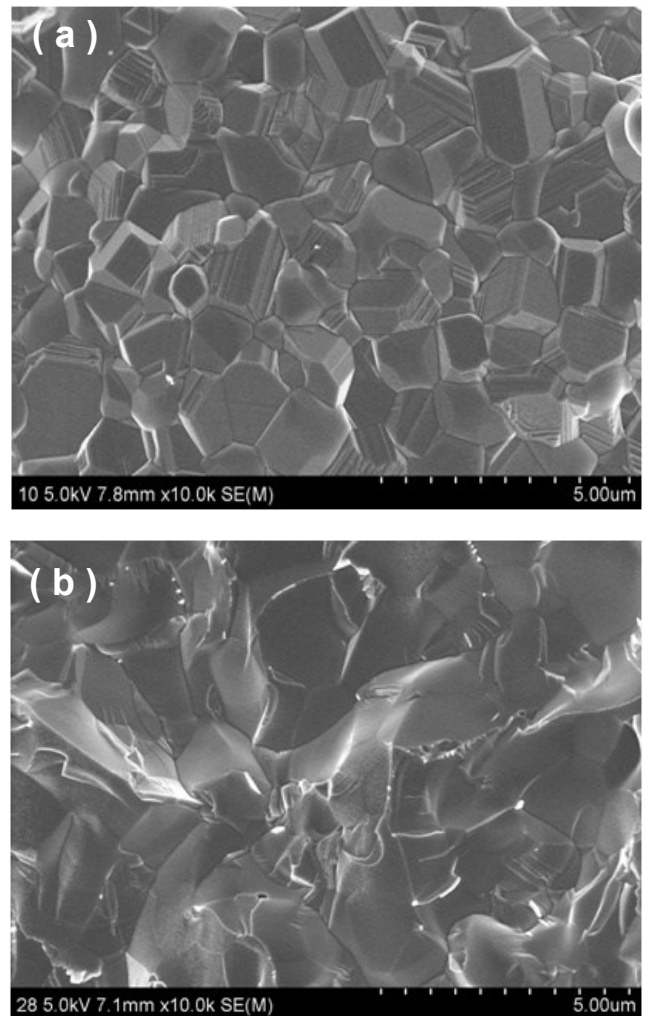


Figure 3. SEM images of cross section of (a) $Y_{0.2}Al_{0.1}Mn_{0.27}Fe_{0.16}Ni_{0.27}O_x$ and (b) $Y_{0.2}Al_{0.1}Mn_{0.264}Fe_{0.16}Ni_{0.264}Cr_{0.012}O_x$.

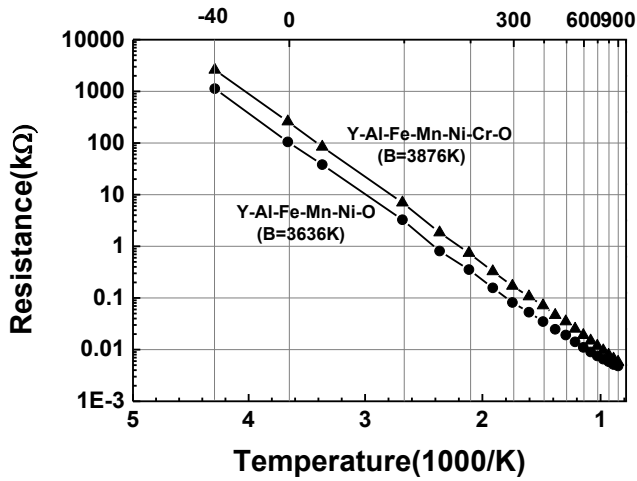


Figure 4. Resistance behaviors with the reciprocal of the absolute temperature.

The microstructures without pores grain boundaries or within grains show the best sintering effect for high densification to each.

Fig.4 shows plots of the resistance against the reciprocal of the absolute temperature ($1/T$) for the system Y-Al-Mn-Fe-Ni-O NTC thermistors with or without Cr_2O_3 content. The resistance decreases exponentially with temperature. It is found that the NTC thermistors operate steadily with the straight line relationship between the electrical resistance and the temperature over a wide temperature range, indicating NTC thermistor characteristics.

The slope of resistivity versus $1/T$ curve is taken generally as a measure of the activation energy of conductivity. In the case of thermistor, the slope of resistance versus $1/T$ is the B constant, sometimes called the coefficient of temperature sensitivity.

$$B_{T_1/T_2} = \frac{\ln(R_1/R_2)}{1/T_1 - 1/T_2} \quad (1)$$

Where R_1 and R_2 are the resistances measured at the absolute temperature of T_1 and T_2 , respectively.

The B constant between 0°C and 600°C is 3636K for $\text{Y}_{0.2}\text{Al}_{0.1}\text{Mn}_{0.27}\text{Fe}_{0.16}\text{Ni}_{0.27}\text{O}_x$ and 3876K for $\text{Y}_{0.2}\text{Al}_{0.1}\text{Mn}_{0.264}\text{Fe}_{0.16}\text{Ni}_{0.264}\text{Cr}_{0.012}\text{O}_x$. The resistance at 0°C and 600°C is measured $100\text{k}\Omega$ and $9\ \Omega$ for $\text{Y}_{0.2}\text{Al}_{0.1}\text{Mn}_{0.27}\text{Fe}_{0.16}\text{Ni}_{0.27}\text{O}_x$ and $300\text{k}\Omega$ and $12\ \Omega$ for $\text{Y}_{0.2}\text{Al}_{0.1}\text{Mn}_{0.27}\text{Fe}_{0.16}\text{Ni}_{0.27}\text{Cr}_{0.01}\text{O}_x$, respectively. The mixture of refractory oxides and transition metal oxides extend the measure range from 0°C to 600°C and the addition of Cr_2O_3 increase the resistance and the B constant.

These phenomena could be explained to the change of microstructure and activation energy of conduction carriers. Generally, the resistance is increased with the size decrement of grains for a sintered ceramics because the grain boundaries could be the scattering centers of the conduction carriers. The grain size and the total length of grain boundaries for a

sintered ceramics are in inverse proportion to each other, as shown in Figure 3. Although the grain sizes of $\text{Y}_{0.2}\text{Al}_{0.1}\text{Mn}_{0.264}\text{Fe}_{0.16}\text{Ni}_{0.264}\text{Cr}_{0.012}\text{O}_x$ are bigger than those of $\text{Y}_{0.2}\text{Al}_{0.1}\text{Mn}_{0.27}\text{Fe}_{0.16}\text{Ni}_{0.27}\text{O}_x$, the resistance of the former is high. It means that the resistance difference could not relate to the scattering effect at the grain boundaries for the conduction carriers.

The reason for the dependence of the B constant on these Y-Al-Mn-Fe-Ni-Cr-O systems is not still clear at present. To elucidate the properties of the B constant and the electrical behaviors, further investigation will be necessary, i.e., exact carrier type and concentration, the analysis of micro- and crystal-structure, and the consideration of defect chemistry and structure of the samples.

The further analyses for the difference of the electrical resistance and the B constant will be reported at the conference.

IV. CONCLUSION

The mixtures of refractory oxides like Y_2O_3 , Al_2O_3 , and transition metal oxides like MnO_2 , Fe_2O_3 , NiO , and Cr_2O_3 powders were prepared by normal ceramic processing for the composition of $\text{Y}_{0.2}\text{Al}_{0.1}\text{Mn}_{0.27}\text{Fe}_{0.16}\text{Ni}_{0.27}\text{O}_x$ and $\text{Y}_{0.2}\text{Al}_{0.1}\text{Mn}_{0.264}\text{Fe}_{0.16}\text{Ni}_{0.264}\text{Cr}_{0.012}\text{O}_x$. The sintered specimens have high densification and good properties of NTC thermistors. With the addition of Cr_2O_3 as a dopant, the crystallinity and the grain size were decreased and increased, respectively. The resistance decreases exponentially with temperature. The specimens show the straight line relationship between the electrical resistance and the temperature over a wide temperature range, indicating NTC thermistor characteristics. Additionally, these systems extend the measurement range of NTC thermistor from 0°C to 600°C .

ACKNOWLEDGMENT

This research was Supported by Basic Science Research Program through the National Research Foundation(NRF) of Korea funded by the Ministry of Education(2014-025966).

REFERENCES

- [1] J. A. Becker, C. B. Green, G. L. Pearson, "Properties and uses of thermistors thermally sensitive resistors", Am. Inst. Elect. Eng. Trans., Vol. 65(11), pp 711-725, 1946.
- [2] S. A. Kanade, V. Puri, "Composition dependent resistivity of thick film $\text{Ni}_{(1-x)}\text{Co}_x\text{Mn}_2\text{O}_4$ ($0 \leq x \leq 1$) NTC thermistors", Materials Letters, vol. 60, pp. 1428-1431, 2006.
- [3] D. Houivet, J. Bernard, J. M. Haussonne, "High temperature NTC ceramic resistors (ambient-1000°C)", J. European Ceram. Soc., vol. 24, pp.1237-1241, 2004.
- [4] A. Banerjee, S.A. Akbar, "A new method for fabrication of stable and reproducible yttria-based thermistors", Sen. and Actuators, vol. 87, pp. 60-66, 2000.
- [5] G. Lavenuta, "Negative temperature coefficient thermistors" Sensors, vol.14, pp46-55, 1997.
- [6] J. G. Fagan, V. R. W. Amarkoon, "Reliability and reproducibility of ceramic sensors: Part I NTC thermistor" Am. Ceram. Soc. Bull. 72, pp70-78, 1993.

- [7] K. Park, S. J. Yun, "Effect of SiO₂ addition on the electrical stability of (Mn_{2.1-x}Ni_{0.9}Si_x)O₄ (0 ≤ x ≤ 0.18) negative temperature coefficient thermistors", *Mater. Lett.*, vol. 58, pp933-937, 2004.
- [8] B. Gillot, J. L. Baudour, F. Bouree, et al., "Ionic configuration and cation distribution in cubic nickel manganite spinels Ni_xMn_{3-x}O₄ (0.57 < x < 1) in relation with thermal histories, *Solid State Ionics*, vol. 58, pp155-161, 1992.
- [9] K. Park, "Microstructure and electrical properties of Ni_{1.0}Mn_{2-x}Zr_xO₄ (0 ≤ x ≤ 1.0) negative temperature coefficient thermistors" *Mater. Sci. Eng. B*, vol 104, pp9-14, 2003.
- [10] J. L. M. Vidales, P. Garcia-Chain, R. M. Rojas, E. Vila, O. Garcia-Martinez, "Preparation and characterization of spinel type Mn-Ni-Co-O negative temperature coefficient ceramic thermistors", *J. Mater. Sci.*, Vol. 33, pp1491-1496, 1998.
- [11] R. N. Jadhav, V. Puri, "Influence of copper substitution on structural, electrical and dielectric properties of Ni_(1-x)Cu_xMn₂O₄ (0 ≤ x ≤ 1) ceramics", *J. of Alloys and Compounds*, vol.507, pp.151-156, 2010.
- [12] R. N. Jadhav, S. N. Mathad, V. Puri, "Studies on the properties of Ni_{0.6}Cu_{0.4}Mn₂O₄ NTC ceramic due to Fe doping", *Ceram. International*, vol.38, pp. 5181-5188, 2012.
- [13] A. Feltz, W. Polzl, "Spinel forming ceramics of the system Fe_xNi_yMn_{3-x-y}O₄ for high temperature NTC thermistor applications", *J. Eur. Ceram. Soc.*, vol. 20, pp2353-2366, 2000.
- [14] X. Li, Y. Luo, X. Li, "Preparation and electrical properties of perovskite ceramics in the system BaBi_{1-x}Sb_xO₃ (0 ≤ x ≤ 0.5)" *J. of Alloys and compounds*, vol. 509, pp.5373-5375, 2011.
- [15] Y. Luo, X. Liu, "High temperature NTC BaTiO₃-base ceramic resistors", *Mat. Letters*, vol. 59, pp. 3881-3884, 2005.
- [16] G. H. Jin, G. P. Choi, W. Y. Lee, and J. S. Park, "Gas Sensing Property of Perovskite SrTi_{1-x}Fe_xO₃ Fabricated by Thick Film Planar Technology", *J. of Nanoscience and Nanotechnology*, vol. 11, pp.1738-1741, 2011.
- [17] W. Y. Lee, D. M. Na and J. S. Park, "Planar sensor properties of perovskite Sr(Ti_{1-x}Fe_x)O_{3-δ} powders prepared by a sol gel Method" *J. of Ceram. Processing Research*. vol. 13(6), pp. 717-720, 2012.
- [18] S. H. Choi, S. J. Choi, B. K. Min, W. Y. Lee, J. S. Park, I. D. Kim, "Facile Synthesis of p-type Perovskite SrTi_{0.65}Fe_{0.35}O_{3-δ} Nanofibers Prepared by Electrospinning and Their Oxygen-Sensing Properties", *Macromol. Mater. Eng.*, vol. 298(5), pp.521-527, 2013.
- [19] G. Thornton, B.C. Tofield, D.E. Williams, "Spin state equilibria and the semiconductor to metal transition of LaCoO₃", *Solid State Commun.*, vol.44, pp1213, 1982.
- [20] K. Asai, A. Yokokura, J.M. Tranquada, et al., "Two spin-state transitions in LaCoO₃", *J. Phys. Soc. Jpn.*, vol. 67, pp290, 1998.